



**HAL**  
open science

# Ultrafast Rotational and Translational Energy Relaxation in Neat Liquids

Jakob Petersen, Klaus Møller, James Hynes, Rossend Rey

► **To cite this version:**

Jakob Petersen, Klaus Møller, James Hynes, Rossend Rey. Ultrafast Rotational and Translational Energy Relaxation in Neat Liquids. *Journal of Physical Chemistry B*, 2021, 125 (46), pp.12806-12819. 10.1021/acs.jpcc.1c08014 . hal-04005999

**HAL Id: hal-04005999**

**<https://ens.hal.science/hal-04005999>**

Submitted on 4 Mar 2024

**HAL** is a multi-disciplinary open access archive for the deposit and dissemination of scientific research documents, whether they are published or not. The documents may come from teaching and research institutions in France or abroad, or from public or private research centers.

L'archive ouverte pluridisciplinaire **HAL**, est destinée au dépôt et à la diffusion de documents scientifiques de niveau recherche, publiés ou non, émanant des établissements d'enseignement et de recherche français ou étrangers, des laboratoires publics ou privés.



## Ultrafast Rotational and Translational Energy Relaxation in Neat Liquids

Petersen, Jakob; Møller, Klaus B.; Hynes, James T.; Rey, Rossend

*Published in:*

Journal of Physical Chemistry Part B: Condensed Matter, Materials, Surfaces, Interfaces & Biophysical

*Link to article, DOI:*

[10.1021/acs.jpcc.1c08014](https://doi.org/10.1021/acs.jpcc.1c08014)

*Publication date:*

2021

*Document Version*

Peer reviewed version

[Link back to DTU Orbit](#)

*Citation (APA):*

Petersen, J., Møller, K. B., Hynes, J. T., & Rey, R. (2021). Ultrafast Rotational and Translational Energy Relaxation in Neat Liquids. *Journal of Physical Chemistry Part B: Condensed Matter, Materials, Surfaces, Interfaces & Biophysical*, 125(46), 12806–12819. <https://doi.org/10.1021/acs.jpcc.1c08014>

---

### General rights

Copyright and moral rights for the publications made accessible in the public portal are retained by the authors and/or other copyright owners and it is a condition of accessing publications that users recognise and abide by the legal requirements associated with these rights.

- Users may download and print one copy of any publication from the public portal for the purpose of private study or research.
- You may not further distribute the material or use it for any profit-making activity or commercial gain
- You may freely distribute the URL identifying the publication in the public portal

If you believe that this document breaches copyright please contact us providing details, and we will remove access to the work immediately and investigate your claim.

# Ultrafast rotational and translational energy relaxation in neat liquids

Jakob Petersen\*

*Department of Chemistry, Technical University of Denmark, Kemitorvet 207, 2800 Kgs. Lyngby, Denmark  
(Present address: Nordea Bank Denmark, Department of Model Risk, Grønvej 10, 2300 Copenhagen, Denmark)*

Klaus B. Møller†

*Department of Chemistry, Technical University of Denmark, Kemitorvet 207, 2800 Kgs. Lyngby, Denmark*

James T. Hynes‡

*Department of Chemistry, University of Colorado, Boulder, Colorado 80309, United States  
PASTEUR, Department of Chemistry, École Normale Supérieure,  
PSL University, Sorbonne Université, CNRS 75005 Paris, France*

Rosend Rey§

*Departament de Física, Universitat Politècnica de Catalunya, Campus Nord B4-B5, Barcelona 08034, Spain  
(Dated: October 24, 2021)*

**ABSTRACT:** The excess energy flow pathways during rotational and translational relaxation induced by rotational or translational excitation of a single molecule of and within each of four different neat liquids ( $\text{H}_2\text{O}$ ,  $\text{MeOH}$ ,  $\text{CCl}_4$ , and  $\text{CH}_4$ ) are studied using classical molecular dynamics simulations and energy flux analysis. For all four liquids, the relaxation processes for both types of excitation are ultrafast, but the energy flow is significantly faster for the polar, hydrogen-bonded (H-bonded) liquids  $\text{H}_2\text{O}$  and  $\text{MeOH}$ . Whereas the majority of the initial excess energy is transferred into hindered rotations (librations) for rotational excitation in the H-bonded liquids, an almost equal efficiency for transfer to translational and rotational motions is observed in the nonpolar, non-H-bonded liquids  $\text{CCl}_4$  and  $\text{CH}_4$ . For translational excitation, transfer to translational motions dominates for all liquids. In general, the energy flows are quite local, i.e., more than 70 % of the energy flows directly to the first solvent shell molecules, reaching almost 100 % for  $\text{CCl}_4$  and  $\text{CH}_4$ . Finally, the determined validity of linear response theory for these nonequilibrium relaxation processes is quite solvent-dependent, with the deviation from linear response most marked for rotational excitation and for the nonpolar liquids.

## I. INTRODUCTION

The mechanisms and rates of nonequilibrium energy relaxation in liquids are obviously key for many reaction and transport processes. Typically, the ultrafast relaxation dynamics of liquids are experimentally and/or computationally/theoretically studied via electronic or vibrational pumping of a foreign solute dissolved in the liquid, and the subsequent spectroscopic probing of that solute, or the surrounding liquid itself. The former, typically involving an electronically excited dye molecule or reaction system (see e.g. Refs. 1,2 and the extensive list in Ref. 3), largely falls under the rubric of “solvation dynamics”. The latter (see e.g. Refs. 4,5) is often (though not exclusively<sup>6</sup>) focused on vibrational energy transfer and relaxation of the solute, i.e. (in quantum language) the population dynamics of the solute’s vibrational state.

Our exclusive focus here is instead on “intramural” relaxation, i.e. neat liquid dynamics induced by excitation (here rotational or translational) of one of the liquid’s molecules, rather than a foreign solute. The motivation of this choice has several aspects. First, a number of recent experiments have examined ultrafast dynamics in neat liquids (so far, almost all in neat water<sup>7–10</sup>) via terahertz (THz) or x-ray excitations and dynamics, with spatial aspects of the liquid’s resulting rotational

and translational response subsequently probed via x-ray scattering techniques. Second, the analysis of ultrafast x-ray scattering experiments involving excitation of foreign probes requires as well attention to the interpretation of spatial and dynamical aspects of the surrounding liquid itself.<sup>12,13</sup> Third, the novel and exciting possibility of controlled motion in liquids, e.g. through self-thermophoresis,<sup>14</sup> requires comprehension of energy flow in the liquid itself.

In all these arenas, the temporal/spatial evolution of the liquid requires characterization—most especially when x-rays are involved—and the work/energy flow framework that we employ here addresses precisely those aspects, at a molecular level. In particular, here we employ the energy flow (flux) analysis introduced by Gertner, Whitnell, Wilson and Hynes<sup>15,16</sup> (and framed in a more general context in 17 by Rey and Hynes) to provide a description of the energy flows associated with relaxation resulting from rotational and translational excitation of a single molecule belonging to and within each one of for a set of four neat liquids. This range from the polar and hydrogen-bonded (H-bonded) liquids water  $\text{H}_2\text{O}$  and methanol  $\text{MeOH}$  to nonpolar liquids carbon tetrachloride  $\text{CCl}_4$  and (high density) supercritical methane  $\text{CH}_4$  (the latter chosen to reduce the intermolecular interactions). This work follows the contributions of

1 corresponding energy flow studies of relaxation dynam-  
2 ics subsequent to molecular vibrational,<sup>17,18</sup> rotational,<sup>19</sup>  
3 and electronic<sup>3,20–23</sup> excitations in aqueous solution or  
4 pure water by several of us, and to vibrational studies  
5 by others.<sup>24–27</sup> The analysis of energy flows has several  
6 attractive features,<sup>15–27</sup> the most important of which is  
7 the ability to follow at a molecular level the pathways  
8 and timescales of the flow of energy, both directly in a  
9 nonequilibrium framework such that short-lived motions  
10 can be followed, and in a fashion devoid of cross terms  
11 which greatly complicates analysis in equilibrium time  
12 correlation function approaches.

13 In the present contribution, we exploit aspects of this  
14 methodology to delve more deeply into rotational and  
15 translational energy relaxation, topics both relatively lit-  
16 tle studied compared to electronic and vibrational excita-  
17 tions (see e.g. Refs. 18,19,28–47). These are intertwined  
18 processes, in that one type of energy excitation will lead  
19 to a combination of both types of energy flows. We will  
20 start by expanding our previous study of the relaxation of  
21 an initial rotational excitation in water,<sup>19</sup> thus broaden-  
22 ing its scope, and, further, extend this approach to other  
23 neat liquids listed above, namely methanol, carbon tetra-  
24 chloride and methane; one aim here is to assess the gener-  
25 ality of the findings for water, by means of a comparative  
26 study with progressively less associated molecular liq-  
27 uids. The present analysis certainly does not exploit all  
28 aspects of the energy flow for these liquids, which would  
29 require considerably further discussion, left for the future  
30 (e.g. elucidation of the electronic excitation-induced en-  
31 ergy flow has required a number of publications<sup>3,20–23</sup>).  
32 Rather we focus on exposing a number of principal fea-  
33 tures of the energy flows in these liquids, including their  
34 main similarities and contrasts.

35 We recall for perspective that in the earlier effort<sup>19</sup>  
36 the energy flow in the relaxation of a rotationally excited  
37 water molecule was characterized by several key features:  
38 overwhelming transfer into the neighboring molecules' li-  
39 brations (hindered rotational motions), i.e., transfer into  
40 translations is a minority channel; non-negligible contri-  
41 bution of direct transfer into water molecules beyond  
42 the first hydration shell, i.e., to those not in direct con-  
43 tact with the excited H<sub>2</sub>O molecule; ultrafast dynamics  
44 (sub-100 fs), and resilience of the linear response with al-  
45 most negligible differences between equilibrium dynamics  
46 and nonequilibrium relaxation after excitations of tens of  
47  $k_B T$ . Each one of these rotational excitation aspects is  
48 probed for each liquid in the present work, with a special  
49 eye on discerning the role that hydrogen bonding plays in  
50 the differences. In addition, the linear response resilience  
51 aspect is probed via both equilibrium and nonequilib-  
52 rium simulations to explore possible breakdowns of linear  
53 response. A number of such breakdowns are known  
54 in the case of electronic excitations,<sup>48–51</sup> with a notable  
55 occurrence for rotational excitations in the excited solute-  
56 solvent work of Stratt and coworkers<sup>28–30</sup> (see also Ref.  
57 42); this is related to the present effort, although here we  
58 employ the novel energy flow perspective and focus on

neat liquids.

An additional major issue addressed here is the character of the energy flow in the relaxation of molecular translational excitations, a topic which has received relatively little attention.<sup>31,33,34,46</sup> (This contrasts with the extensive gas phase effort;<sup>35</sup> this lacuna in part due to the blurring in the condensed phase of rotational transitions,<sup>36</sup> with its associated loss of spectroscopic information). But regard this neglect as unwarranted, even beyond the feature that assorted chemical reactions will require and excite surrounding solvent translations in the passage through transition states.<sup>16,28–30,42–44</sup> In connection with the present work's topic it is evident—as we have implied above—from energy flow analysis that there is a non-negligible interplay between translations and rotations, with substantial and rapid energy exchange (already evident for water in Ref. 19), and consequently, a full understanding requires consideration of both simultaneously.

Energy exchange between rotations and translations will pervade our account, e.g. rotational (translational) excitation resulting in translational (rotational) energy flows. This focus differs from the extensive prior work on translational-rotational coupling which, in its liquid phase aspects, largely focused on diffusive transport aspects, with differing conclusions on the magnitude of the coupling there.<sup>35,37–40</sup> Our energy flow perspective focuses on a time scale (sub-100 fs) roughly one order of magnitude shorter than in previous work. As shown here and in Ref. 19, a strong energy flux coupling exists; here the impact of the exchange's ultrafast character on the coupling (and the associated rapid thermalization) may notably differ from coupling aspects probed via diffusion at longer time scales.

The remainder of this paper is organized as follows: In Section II, we briefly review the relevant formulas for energy flow analysis of translational/rotational energy relaxation of rigid molecules, while Section III presents the computational details of the equilibrium and non-equilibrium classical molecular dynamics simulations. In Section IV, the results for rotational and translational energy dynamical relaxation, and associated energy flow pathways and timescales, in water, methanol, carbon tetrachloride, and methane are presented and discussed, and we offer some concluding remarks in Section V.

## II. ENERGY FLUX ANALYSIS

The basic formalism to be used for the analysis of the energy fluxes, responsible for and accompanying the relaxation, is the Poisson bracket formalism developed in Ref. 17. Here we focus on the excess energy transfer from one initially excited molecule — the  $i$ 'th molecule — to the surrounding neighbor molecules. The starting point for the flow description is the partitioning of the full Hamiltonian

$$H = H_i + U + H_{\text{rest}}, \quad (1)$$

where  $H_i$  is the sum of kinetic and intramolecular potential energy of the  $i$ 'th molecule,  $U$  denotes the intermolecular potential energy due to the interactions between the  $i$ 'th molecule and the rest of the molecular system, and the remaining kinetic and potential energy terms are contained in  $H_{\text{rest}}$ . In the case of rigid molecules (which we employ in the simulations),  $H_i = K_{T,i} + K_{R,i}$ , where  $K_{T,i}$  and  $K_{R,i}$  are the translational and rotational kinetic energies of the  $i$ 'th molecule, respectively.

In the Poisson bracket notation,<sup>17</sup> the energy flows, or powers, associated with each of  $K_{T,i}$ ,  $K_{R,i}$ , and  $U$  are given by

$$\begin{aligned} \frac{dK_{T,i}}{dt} &= [K_{T,i}, H] = [K_{T,i}, U]; \\ \frac{dK_{R,i}}{dt} &= [K_{R,i}, H] = [K_{R,i}, U]; \\ \frac{dU}{dt} &= [U, H] = [U, K_{T,i}] + [U, K_{R,i}] + [U, H_{\text{rest}}], \end{aligned} \quad (2)$$

which lead directly to the kinetic energy time dependence relation

$$\frac{dK_{T,i}}{dt} + \frac{dK_{R,i}}{dt} = -\frac{dU}{dt} + [U, H_{\text{rest}}]. \quad (3)$$

With the definition of the Poisson bracket and the assumption that  $U$  is a function of particle positions only, the last term in Eq. (3) can be written as

$$[U, H_{\text{rest}}] = \sum_{j\beta} \frac{\partial U}{\partial \mathbf{q}_{j\beta}} \cdot \frac{\partial H_{\text{rest}}}{\partial \mathbf{p}_{j\beta}} = -\sum_{j\beta} \mathbf{F}_{j\beta,i} \cdot \mathbf{v}_{j\beta}, \quad (4)$$

where we use the Cartesian phase space coordinates ( $\{\mathbf{p}_{j\beta}\}, \{\mathbf{q}_{j\beta}\}$ ) of the constituent atoms (or interaction sites) of the molecular system.  $\mathbf{F}_{j\beta,i}$  denotes the force on atom  $j\beta$  of molecule  $j$  due to the interaction with the  $i$ 'th molecule, and  $\mathbf{v}_{j\beta}$  is the Cartesian velocity vector of atom  $j\beta$ .

From Eq. (3), we see that the variation of the sum of the translational and rotational kinetic energies of molecule  $i$  in time can be partitioned into two terms: (1) a change in intermolecular potential energy due to the interactions between the  $i$ 'th molecule and the remaining ones, and (2) the powers associated with rotational and translational motions of each molecule.

In order to effect such rotation/translation partition, we first write the atomic velocity of atom  $j\beta$  as  $\mathbf{v}_{j\beta} = \mathbf{v}_j + \boldsymbol{\omega}_j \times \mathbf{r}_{j\beta}$ , where  $\mathbf{v}_j$  and  $\boldsymbol{\omega}_j$  are the center-of-mass and angular velocity of molecule  $j$ , respectively, and  $\mathbf{r}_{j\beta}$  is the position of atom  $j\beta$  with respect to the center-of-mass position of molecule  $j$ . This allows us to recast Eq. (4) in the form

$$[U, H_{\text{rest}}] = -\sum_j (\mathbf{F}_{j,i} \cdot \mathbf{v}_j + \boldsymbol{\tau}_{j,i} \cdot \boldsymbol{\omega}_j), \quad (5)$$

where  $\mathbf{F}_{j,i}$  and  $\boldsymbol{\tau}_{j,i}$  are the force and torque (with respect to the molecular center-of-mass position) on molecule  $j$  due to the interaction with the  $i$ 'th molecule.

These relations then lead to the key ‘‘work’’ expression which governs the rotational or translational energy flow when integration over time on both sides of Eq. (3) is carried out

$$\Delta K_{T,C} + \Delta K_{R,C} = -\Delta U - W_T - W_R, \quad (6)$$

where we have substituted  $C$  for  $i$ , since we will henceforth refer to the  $i$ 'th molecule, i.e., the rotationally/translationally excited molecule, as the ‘‘central’’ molecule and the rest of the liquid molecular system as solvent, or neighboring, molecules. The five terms in Eq. (6) are defined as follows:  $\Delta K_{T,C}$  and  $\Delta K_{R,C}$  are respectively the changes in translational and rotational kinetic energies of the central molecule between the times  $t$  and zero, and  $\Delta U$  is the change in potential energy due to the interactions between the central molecule and the solvent molecules in the same time interval. The work, or time-integrated power, terms  $W_T$  and  $W_R$  denote respectively the work on translation and rotation of the solvent molecules due to the interactions with the central molecule

$$\begin{aligned} W_T &= \int_0^t ds \mathbf{F}_{j,C}(s) \cdot \mathbf{v}_j(s) \\ W_R &= \int_0^t ds \boldsymbol{\tau}_{j,C}(s) \cdot \boldsymbol{\omega}_j(s), \end{aligned} \quad (7)$$

where both work terms can be partitioned into groups of solvent molecules, e.g., different solvent shells surrounding the central excited molecule. Thereby, the ‘‘locality’’ of the energy flow during the relaxation processes can be determined — by partitioning the two work terms — and the motions, into which the excess translational/rotational kinetic energy flows, can be identified — directly from the work terms.

### III. SIMULATION METHODS

Equilibrium and non-equilibrium classical molecular dynamics simulations of 216 rigid molecules in a cubic box are carried out with an in-house code, which applies periodic boundary conditions and the minimum image convention. The equations of motion for the constraint dynamics are solved with the RATTLE algorithm<sup>52</sup> using a time step of 1 fs, and the Nosé-Hoover thermostat<sup>53,54</sup> is applied in the  $NVT$  simulations at  $T = 300$  K for each system. The force cutoff distance is chosen as half the cubic box length, and the Ewald summation correction for the Coulomb forces has been included. The SPC/E<sup>55</sup> model is used for water, the OPLS parameters are chosen for methanol<sup>56</sup> and methane,<sup>57</sup> and the force field due to Rey *et al.*<sup>58</sup> is used to model carbon tetrachloride. The density  $\rho$  of each liquid is given in Table I. (Methane would be supercritical, albeit with the high density characteristic of the corresponding liquid at atmospheric pressure).

TABLE I: Density, principal moments of inertia, angular frequencies, and rotational periods for the four neat liquids. The density unit is  $\text{g}/\text{cm}^3$ , the unit of the principal moments of inertia is  $\text{u}\cdot\text{\AA}^2$ , the angular frequencies unit is  $\text{cm}^{-1}$ , and the rotational period unit is fs.

	$\rho$	$I_{xx}$	$I_{yy}$	$I_{zz}$	$\omega_x^{\text{rms}}$	$\omega_y^{\text{rms}}$	$\omega_z^{\text{rms}}$	$T_x$	$T_y$	$T_z$
H <sub>2</sub> O	0.998	0.5964	1.344	1.941	108.6	72.31	60.18	307.2	461.3	554.2
MeOH	0.787	0.7371	16.86	17.60	97.66	20.42	19.99	341.6	1633	1669
CCl <sub>4</sub>	1.58	294.8	294.8	294.8	4.883	4.883	4.883	6831	6831	6831
CH <sub>4</sub>	0.406	3.194	3.194	3.194	46.92	46.92	46.92	710.9	710.9	710.9

For all of these molecular systems 10,000 sets of initial conditions are produced from several equilibrium  $NVT$  simulation runs, where snapshots of phase space points are saved every 2 ps. In each case, the set of initial conditions corresponds to a canonical ensemble at  $T \approx 300$  K with a standard deviation of  $\sim 11$ -12 K. (Having the same temperature for all four systems greatly facilitates comparison, as equilibrium thermal kinetic energies are identical).

Based on these initial conditions, equilibrium and non-equilibrium  $NVE$  simulation runs are carried out (the  $NVE$  conditions are chosen to avoid non-collisional force adjustments due to the thermostat<sup>53,54</sup>). In the non-equilibrium runs, the central molecule is either translationally or rotationally excited at time zero. These excitation processes are discussed next.

### A. Translational excitation

The instantaneous translational excitation of the central molecule is simply modeled by adding the positive scalar  $v = \sqrt{2E_{\text{ex}}/M_C}$  to the  $x$ -component (chosen arbitrarily) of the center-of-mass velocity vector  $\mathbf{v}_C$ . Here  $E_{\text{ex}}$  denotes the translational excitation energy, and  $M_C$  is the mass of the central molecule. Since the  $x$ -component of  $\mathbf{v}_C$  can already have any real value at time zero, the initial translational excitation energy is not equal to  $E_{\text{ex}}$  for each trajectory, but, on average, the excess (i.e. above thermal) translational kinetic energy of the central molecule at time zero is  $E_{\text{ex}}$ , i.e., the Maxwell-Boltzmann distribution, for the  $x$ -component of  $\mathbf{v}_C$  at time zero, is centered around  $v$ .

### B. Rotational excitation

In a similar fashion, the instantaneous rotational excitation of the central molecule is modeled by adding the positive scalar  $v_i = \sqrt{2E_{\text{ex}}/I_{ii}}$  to the angular velocity component associated with the principal  $i$ -axis. Here  $E_{\text{ex}}$  denotes the rotational excitation energy, and  $I_{ii}$  is the principal moment of inertia element associated with the  $i$ -axis. Similarly to the translational case, the initial rotational excitation energy is not equal to  $E_{\text{ex}}$  for each trajectory, but, on average, the excess rotational kinetic energy of the central molecule at time zero is  $E_{\text{ex}}$ . For

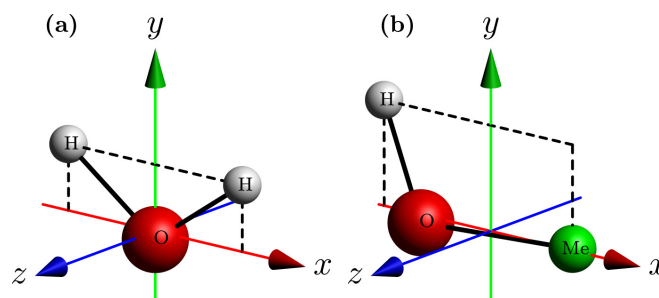


FIG. 1: Principal axes for SPC/E water (a) and OPLS methanol (b).

the asymmetric water and methanol molecules, we will investigate how the rotational relaxation depends on the excitation axis, i.e. the rotational excitation is carried out, with respect to each of the principal axes in turn, by changing the angular velocity with respect to the principal axis in question. The principal moment of inertia elements are given in Table I, together with the associated root-mean-square angular frequency ( $\omega_i^{\text{rms}} = \sqrt{k_B T / I_{ii}}$ ) and rotational period ( $P_i = 2\pi / \omega_i^{\text{rms}}$ ) for free rotation at  $T = 300$  K. Here we have chosen the notation system in which the principal axes are denoted according to ascending moments of inertia, i.e.,  $I_{xx} \leq I_{yy} \leq I_{zz}$ . The water and methanol molecules' principal axes are shown in Fig. 1. Obviously, the principal moments of inertia are identical for the spherical top molecules CCl<sub>4</sub> and CH<sub>4</sub>.

## IV. RESULTS AND DISCUSSION

### A. Rotational kinetic energy relaxation

First we examine the rotationally excited central molecule's rotational kinetic energy during the relaxation process. Figure 2 shows, as a function of time, this molecule's normalized excess rotational kinetic energy after a 1 kcal/mol excitation, for each of the four neat liquids (the 1 kcal/mol excitation energy corresponds to the average kinetic energy of a nonlinear rotor  $\langle K_R \rangle \approx 0.894$  kcal/mol at  $T = 300$  K). For H<sub>2</sub>O and MeOH the excitation is along each of the principal axes, while for CCl<sub>4</sub> and CH<sub>4</sub> the relaxation process—when averaged over many trajectories—is independent of the

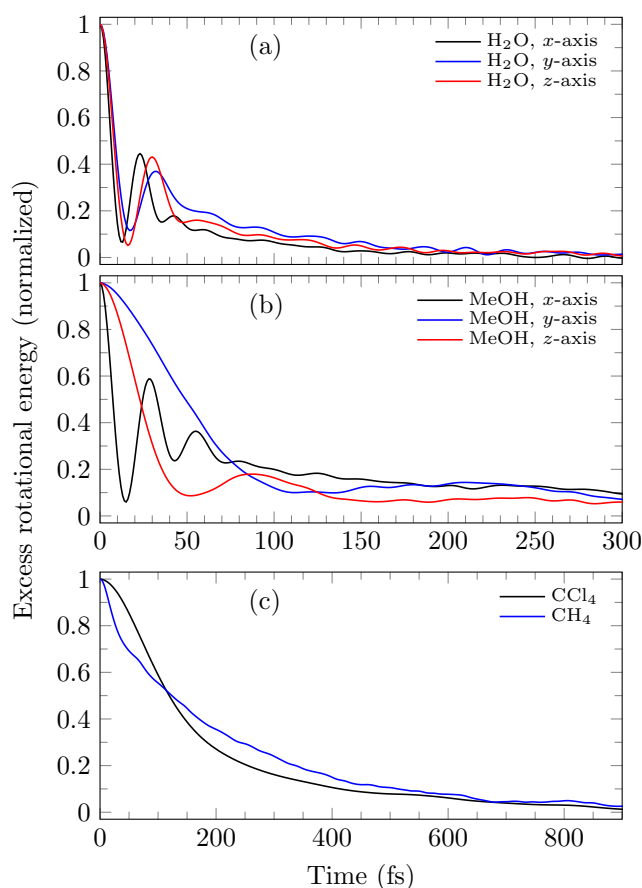


FIG. 2: Normalized excess rotational kinetic energy as a function of time for 1 kcal/mol rotational kinetic energy excitation of a central molecule in each of the four liquids. (a) H<sub>2</sub>O, three principal axes; (b) MeOH, three principal axes; (c) CCl<sub>4</sub> and CH<sub>4</sub>, see the text. Note the change of the time axis in panel (c). (The excess rotational energy is defined as  $\bar{K}_R - \langle K_R \rangle$ , with the first term denoting the nonequilibrium ensemble average of the central excited molecule's rotational kinetic energy, and  $\langle K_R \rangle$  is its equilibrium average which, for nonlinear molecules, is  $\langle K_R \rangle \approx 0.894$  kcal/mol at  $T = 300$  K.)

chosen excitation axis due to the spherical top structure. Rotational relaxation is ultrafast in all cases, essentially complete in less than 1 ps, and significantly faster in the H-bonded liquids. Virtually all of the excess rotational kinetic energy is lost for H<sub>2</sub>O after only  $\sim 200$  fs, independent of the excitation axis and, in the same time interval,  $\sim 85 - 95$  % of the energy is lost for MeOH, while only  $\sim 75$  % and  $\sim 65$  % is lost for CCl<sub>4</sub> and CH<sub>4</sub>, respectively.

The second observation is the presence of oscillations for the two H-bonding liquids in Figs. 2(a) and 2(b), which is completely absent in the two nonpolar (and of course non-H-bonded) liquids in Fig. 2(c), where the relaxation is monotonic. Obviously H-bonding effects are responsible for this division. The oscillatory behavior for water is associated with the rotational “caging” effect,

the halting and reversal of the rotational motion after excitation, i.e., the total torque on the central molecule due to the interactions with the H-bonded neighbors causes the angular momentum vector of the central molecule, on average, to reverse, the conversion of pure rotation to libration. This oscillation feature is of course well known in the context of e.g. the angular momentum time correlation function (TCF). In the kinetic energy context, its occurrence for the rotational kinetic energy TCF, and its connection to a gaussian assumption, was evidently first noted for the isotopic variant, HOD dissolved in D<sub>2</sub>O, in Ref. 47 and later for water itself in Refs. 41 and 19. Oscillatory behavior is also observed for methanol, as expected, but this feature is less pronounced than in water (except for the lowest moment of inertia x-axis excitation case, which involves the central molecules's maximum H motion, see below). This more muted character is likely associated with the dominant H-bonding in methanol involving two H-bonds (rather than four as in water<sup>45,56,59-62</sup>).

We now turn to some more specific details. As we have reported previously,<sup>19</sup> the hindered initial rotational (librational) relaxation in water depends somewhat on the chosen excitation axis, with the damped oscillation frequency largest for the *x*-axis, and smallest for *y*-axis, excitation, see Fig. 2(a).

Figure 2(b) shows that MeOH also exhibits librational oscillations, but – except for the lowest moment of inertia *x*-axis case, for which the MeOH and H<sub>2</sub>O  $I_{xx}$  values are comparable – are markedly slower and more muted than for water. Focusing first on the *x*-axis excitation, the underdamped librational rotational relaxation in methanol is to some degree comparable to the corresponding water excitation case within the first 50 fs, although the return to equilibrium is much slower than for H<sub>2</sub>O. Turning to the *y*- and *z*-axis excitations, the general slowdown compared to the *x*-axis case is consistent with the ratios  $I_{yy}/I_{xx}$  and  $I_{zz}/I_{xx}$  being far greater for MeOH than for H<sub>2</sub>O (cf Table I). But the relative behavior of the *y*- and *z*-axis  $K_R$  decays do not follow such simple ratio expectations:  $I_{zz} > I_{yy}$ , but the *y*-axis decay is noticeably slower. This can be understood in terms of the *y*-axis being nearly parallel to the OH-axis (cf Fig. 1(b)), so that rotation about this axis will be much less hindered.<sup>45</sup> This argument can be made somewhat more detailed by invoking the same initial gaussian behavior for the kinetic energy and angular velocity (or momentum) for MeOH as noted for H<sub>2</sub>O above. Focusing on the angular momentum component  $\mathbf{L}_i$ , the initial gaussian approximation for each of those quantities would give an initial decay proportional to  $(I_{ii}k_bT)^{-1} < \tau_i^2 >$  (which is  $< (d\mathbf{L}_i/dt)^2 > / < \mathbf{L}_i^2 >$ ), the difference between the two axis results being dominated by the different mean square torque, which would be smaller for the *y* axis rotation by the argument above. The similar behavior of the kinetic energy (Fig. 2(b)) and the angular velocity is borne out by the angular velocity TCF results in Ref. 45, which display the same oscillatory and decay charac-

1  
2  
3  
4  
5  
6  
7  
8  
9  
10  
11  
12  
13  
14  
15  
16  
17  
18  
19  
20  
21  
22  
23  
24  
25  
26  
27  
28  
29  
30  
31  
32  
33  
34  
35  
36  
37  
38  
39  
40  
41  
42  
43  
44  
45  
46  
47  
48  
49  
50  
51  
52  
53  
54  
55  
56  
57  
58  
59  
60

teristics as seen in the Fig.2(b)  $K_R$ . Indeed, the authors of Ref. 45 also invoke the nearly parallel  $y$ - and OH-axes to explain the  $y$ -axis angular velocity TCF behavior.

### 1. Energy flow and work.

Now we turn our focus to the time evolution of the energy flow and work terms in Eq. (6) in order to help interpret the observations listed in the previous section and in general, provide a more detailed molecular picture for the dynamics underlying the time evolutions of Fig. 2. We will need to always keep in mind that as the liquid is changed, the excited molecule's identity is changed as well.

Hereafter we will focus the energy flow analysis on a 5 kcal/mol initial rotational kinetic energy excitation. Assorted results for thermal (1 kcal/mol) and higher than 5 kcal/mol excitations, including spatial dependence information, are given in SI. For perspective, the excitations by energies 1-5 kcal/mol correspond to temperatures 600-2000 K of the excited molecule (for a nonlinear rotor) or frequencies 10-50 THz of a photon inducing excitation, e.g., in a pump-probe experiment.

Each of the five terms of the key work Eq. 6 are shown in Fig. 3 for the first 500 fs after the instantaneous rotational excitation along the principal  $x$ -axis of the central molecule. Before recounting the results, we first summarize the variables being presented, focusing on the H<sub>2</sub>O case for illustration.  $\Delta K_{R,C}$  is the magnitude of the rotational energy *lost* by the central molecule C post its initial excitation. This and all variables are normalized by the initial excitation energy; thus, for  $\Delta K_{R,C}$  complete loss equals unity. (The magnitude is used in order to place this variable on the same scale as the remaining variables). Next,  $\Delta U$  is the normalized change in interaction potential energy between C and the remaining molecules of the system. The H<sub>2</sub>O panel for Fig. 3 shows, in the first 20 fs, that C's excess rotational kinetic energy rapidly drops as the interaction potential energy rises. These then both remain strongly correlated in the next 20 fs interval, with different amplitude oscillations, both more slowly decaying thereafter. In the same initial period, the work  $W_R$  done on C's surrounding water molecules rapidly increases, i.e. there is energy flow to the "solvent" waters librational motions. This flow is dominant as very little energy transfer to those waters' translations has occurred:  $W_T$  is very small, though slowly accumulating as time progresses. All this is occurring with little energy transfer to C's translational motion:  $\Delta K_{T,C}$  is even smaller.

Now adopting a more general perspective, we see that for all four liquids, the initial increase in the magnitude  $|\Delta K_{R,C}|$  — i.e., a decrease in the rotational kinetic energy of the central molecule — produces a strong correlated increase in the intermolecular potential energy term  $\Delta U$ , but the magnitude in the initial period 0-40 fs is much greater for the H-bonded liquids. For the lat-

ter H-bonded liquids, the on average initially energetically favorable H-bonded configurations of the central molecule are disrupted by its sudden rotation; for the much more weakly interacting nonpolar liquids, the disruption impact is very much reduced. Here we pause to recount some information available from 58 on energetics for some of our four liquids, which can help to provide perspective on our present results. First, the absolute value of the ratio of the equilibrium average kinetic and potential energies is  $\sim 0.2$  for water and  $\sim 0.33$  for the non-polar liquids. Second, for the ratio of Coulomb to non-Coulomb potential energies, for water the ratio is negative an absolute value  $\sim 0.1$ , while the actual ratio is positive and much less for the non-polar liquids:  $\sim 0.02$  for CCl<sub>4</sub> and  $\sim 0.01$  for methane, both energies being negative in each case.

For both H<sub>2</sub>O and MeOH, the initial oscillatory behavior of  $|\Delta K_{R,C}|$  is largely matched within the first  $\sim 50$  fs by similar oscillations in  $\Delta U$ ; this suggests a description of the local H-bonded "network"—C's neighboring web of H-bonded water molecules—being "stretched/expanded" after C's excitation, then relaxing somewhat at  $t \approx 50$  fs subsequent to the reversal of the C's angular momentum vector, i.e. the rebound of C's caged librational motion. The recovery is significantly smaller for MeOH than for H<sub>2</sub>O, with a much less pronounced energy flow to the solvent librations, and a correspondingly slower relaxation to equilibrium of the potential energy and C's excess rotational kinetic energy.

Turning to the nonpolar liquids, beyond those differences already mentioned above, the most striking features in Fig. 3 are their strong differences from the H-bonded liquids in (a) the efficiency of energy transfer from the rotationally excited central molecule C to the surrounding "solvent" molecules' rotational (librational) motions, and (b) the efficiency of the energy flow to those same molecules' translational modes, revealed both in the kinetic energy changes and the work terms in the Figure.

We focus first on the nonpolar liquids' reduced efficiency of C's rotational kinetic energy transfer to the solvent's rotational motion. The source of this disparity is obviously the absence of the strong intermolecular coupling due to the H-bonds present in H<sub>2</sub>O and MeOH. This comparatively efficient rotational transfer for H<sub>2</sub>O was already reported in Ref. 19. For methanol, such dominant transfer to rotational modes can also be inferred from the rapidly decaying librational oscillatory behavior in Fig. 2(b) for the C's smallest moment of inertia  $x$ -axis excitation: this axis rotation maximizes its—(OH)—hydrogen motion.

The second distinguishing behavior of the nonpolar liquids is very striking: an almost equal transfer efficiency to solvent rotation and translation. The two energy flow work terms  $W_R$  and  $W_T$  build up at rates nearly identical (CCl<sub>4</sub>), or very similar (CH<sub>4</sub>), during the decay of C's rotational kinetic energy. This feature is most likely due to the fact that the transfer of rotational energy of the nearly spherical C molecules to its nearly spherical

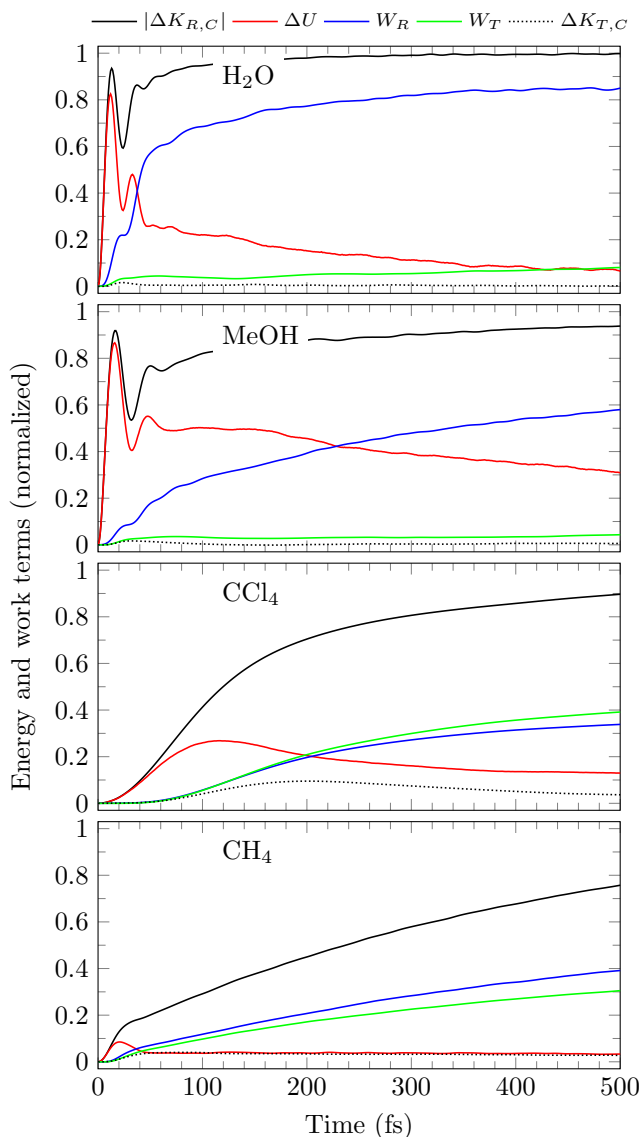


FIG. 3: Normalized (to the initial excitation kinetic energy) energy and work terms for rotational relaxation in the four liquids following instantaneous 5 kcal/mol excitation with respect to the principal  $x$ -axis. Black solid: change in central molecule rotational kinetic energy  $\Delta K_{R,C}$ ; red: potential energy change  $\Delta U$ ; blue: rotational work  $W_R$ ; green: translational work  $W_T$ ; black dotted: change in central molecule translational kinetic energy  $|\Delta K_{T,C}|$ . Further Work results are given in SI Sec. S1.

neighbors primarily requires their relative translational motion.

We can expand somewhat on the above discussion by considering longer time information, whose relevance is evident from the lack of complete energy redistribution and relaxation within the 400 fs time frame of Fig. 3. To this end, we have examined the asymptotic values of the rotational and translational work terms  $W_R$  and  $W_T$  at  $t = 5$  ps, shown in Table II (the first two columns show

TABLE II: Normalized work terms  $W_R$  (energy transferred to rotation) and  $W_T$  (energy transferred to translation) obtained after 5 ps following 5 kcal/mol rotational excitation. The 1st solvent shell is defined to consist of the four nearest molecules. Further Work results are given in SI Sec. S1.

	Solvent		1st solvent shell	
	$W_R$ (%)	$W_T$ (%)	$W_R$ (%)	$W_T$ (%)
H <sub>2</sub> O, $x$	89	11	63	9
H <sub>2</sub> O, $y$	85	15	63	14
H <sub>2</sub> O, $z$	84	16	67	15
MeOH, $x$	83	13	67	12
MeOH, $y$	53	42	41	36
MeOH, $z$	52	43	46	39
CCl <sub>4</sub>	48	51	47	50
CH <sub>4</sub>	56	43	55	41

that 1 – 4 % of the excess energy still resides in  $\Delta U$  at this time)(The Table II results are rounded; the water total percentage is thus less than 0.5 %).

The work entries for the nonpolar liquids CCl<sub>4</sub> and CH<sub>4</sub> confirm the Fig. 3 shorter time behavior of very similar energy flow to the solvent molecules' rotational and translational motion. The energy flows for the H-bonded liquids additionally go beyond the information in Fig. 3 by examination of the axis dependence of the work (Fig. 3 examined solely the principal  $x$  axis case). The MeOH results in Table II's first two columns reveal an overall importance of the energy flow to translation not evident in the  $x$  axis result in Fig. 3. While the ratio  $W_R/W_T$  (for the small moment of inertia  $x$ -axis excitation) is comparable to H<sub>2</sub>O, that ratio is very similar to that for CH<sub>4</sub> for the larger moment of inertia  $y$ - and  $z$ -axis excitation: where  $\sim 53$  % of the excess energy is transferred to rotation and  $\sim 42$  % to translation (and is not greatly different from that of CCl<sub>4</sub>). This dependence on MeOH excitation axis is in line with the observations and our remarks in Sec. IV A.

Finally, for the case of water, with its much less disparate—and all small—moments of inertia, the transfer efficiency of excess energy to rotation and translation of the neighboring molecules is only weakly dependent on the chosen excitation axis, with  $\sim 85$  % of the excess energy transferred to rotation and  $\sim 15$  % to translation (as already shown in Ref. 19, the latter showing a more pronounced energy flow to translation than is evident from Fig. 3). In fact, a simple average of the three excitation results for MeOH,  $\sim 63$  % of the excess energy is transferred to rotation and  $\sim 33$  % to translation, positions MeOH, in terms of energy transfer efficiency, somewhere between the strongly H-bonded H<sub>2</sub>O and the nonpolar liquids. We conclude that the energy flow between rotational and translational modes, while most dominant for the nonpolar liquids, is non-negligible even for the H-bonded liquids.

## 2. Locality of relaxation process.

As pointed out in Section II, the energy flow analysis also allows for a determination of the energy transfer to a subset of the surrounding solvent molecules. Here we do not fully exploit this ability,<sup>18,19</sup> but instead we focus on the energy flow to the first solvent shell. The dominant importance of this first shell is confirmed by graphical comparison of the energy flow results in both SI Secs. S1 and S2, for the complete flows and those to the first shell.

Obviously such a shell needs definition for each liquid. For neat liquid water at  $T = 300$  K and a density of  $\sim 1$  g/cm<sup>3</sup>, this shell comprises four molecules on average, of which two accept bonds from, and two donate H-bonds to, the central water molecule. At the same temperature, but densities of 1.58 g/cm<sup>3</sup> and 0.406 g/cm<sup>3</sup>, the first solvent shell in carbon tetrachloride and methane, based on integration of the C-C radial distribution function up to the first minimum, appears much larger and includes  $\sim 12$  molecules. However, a “sub-shell” containing only four molecules in direct contact with the central molecule can be identified within this first shell,<sup>63,64</sup> for the present energy transfer problem, we adopt this definition for these two nonpolar solvents, for which shorter ranged non-Coulomb interactions dominate, as noted above. Finally, for liquid methanol, at  $T = 300$  K and density of 0.787 g/cm<sup>3</sup>, the first solvent shell is usually assumed, based on integration of the O-O radial distribution function, to contain only two molecules which also corresponds to the averaged number of hydrogen bonds per molecule. However, the central molecule is not completely interlocked between these two neighbors.<sup>56,62</sup> In order to compare the locality of the relaxation processes in terms of solvent shells for the four different liquids, we adopt the convention that the first solvent shell of each liquid contains four molecules. This definition is supported by the determined first shell dominance for the energy flow in methanol found in SI Secs. S1 and S2.

The asymptotic values of the rotational and translation work terms  $W_R$  and  $W_T$ , gauging the energy from the rotationally excited C molecule to the first solvent shell molecules at  $t = 5$  ps, are shown in the last two columns of Table 2. Perhaps the most striking aspect of these flows is the strong distinction in locality between the nonpolar and the H-bonded liquids. The process is very strongly local for the nonpolar liquids CCl<sub>4</sub> and CH<sub>4</sub>, where only  $\sim 2$  % and  $\sim 3$  % of the initial excess energy is transferred to molecules outside the first solvent shell, respectively. By contrast, while the flow to the first shell is still dominant for the H-bonded liquids, the flow is noticeably less local for each axis excitation in water and methanol, typically  $\sim 20$  % of the excitation energy is directly channeled to neighbors beyond the first shell, respectively. Table II gives details of this for results after 5 ps. SI Sec. S1 gives extensive time dependent results comparing total energy flow and the flow to the first shell. (For MeOH, this transfer increases to

$\sim 29 - 47$  %, if the first shell is assumed to consist of only two neighbors, rather than the four included in our definition).

A further feature of interest from Table II is that, for water and methanol, the transfer to translational modes is noticeably more local than the transfer to rotational motions. In the case of water,  $\sim 82-94$  % of the total energy transferred to solvent translational motions is channeled to the first shell, whereas  $\sim 71-80$  % of the total energy transferred to solvent rotational motions goes to rotation of first shell neighbors. This general trend is also observed for methanol, for which these percentages are not dramatically different,  $\sim 86 - 92$  % and  $\sim 81 - 88$  %, respectively.

The increased delocalization of the energy flow from the rotationally excited C molecule in the H-bonded liquids, associated with a degree of coupling beyond the nearest neighbors, is not unexpected, having been already established in detail for water in our previous study.<sup>19</sup> Terms such as “collective”,<sup>20,48,51</sup> (or “network”) are sometimes employed, especially for water, to describe the dynamics of H-bonded solvents. But it is worth again<sup>20</sup> stressing the sobering fact that we still lack a theoretical formulation, e.g. a librational field theory, that would help to more fully characterize dynamical delocalization in H-bonded liquids.

## 3. Linear response investigation.

As we emphasized in the Introduction, the validity of the Linear Response Theory (LRT) approximation, defined below, is important for several related reasons. The first is practical, namely that one can simply use an equilibrium time correlation function to describe the nonequilibrium dynamics. Second, and both of more fundamental and broader significance, is —within the context of the present work—that with suitable normalization, the solvents’ dynamic response to a rotational energy or translational energy excitation, can apply for different sources of those excitations, a feature relevant in connection with the various experiments mentioned in the Introduction.

The remarkable applicability of linear response has been observed for various relaxation processes (e.g., Refs. 2,3,20,20,28,29,41,51,65–67, see Ref. 3 for a more extensive reference list), though some important exceptions exist.<sup>30,49,50,68–70</sup>

These LRT validity observations are largely restricted to electronic excitations, related to time dependent fluorescence experiments. For other types of excitations, an early example of LRT validity for vibrational energy is given in Ref. 71 (see also Ref. 7,15,41). For rotational energy relaxation, we found in the water study<sup>19</sup> that LRT is an adequate description for rotational energy relaxation for a fairly broad range of excitation energies, i.e., the relaxation time was largely independent of the nonequilibrium perturbation’s strength.

Stratt and coworkers found LRT breakdown for relaxation of rapidly rotating solutes, related to a local rotational friction decrease subsequent to a rotationally hot solute-induced first solvent shell expansion.<sup>28–30</sup> Here we will examine, for our selected four neat liquids, the applicability of LRT, and the energy flow pathways dependence, for rotational and translational excitation energies varying over a reasonable range. The LRT results for 1–15 kcal/mol excitations are presented in the text. Much higher energy excitation LRT results are given in the SI, as are all of the detailed energy flow results (beyond those given in Fig. 3 for one excitation energy), with some summary remarks of these SI items also given in the text.

In a standard application of linear response theory, a simple relation is provided for rotational energy relaxation, between the nonequilibrium energy dissipation and the equilibrium rotational energy fluctuations. The nonequilibrium relaxation is conveniently defined by the normalized response function

$$S_R(t) = \frac{\bar{K}_R(t) - \langle K_R \rangle}{\bar{K}_R(0) - \langle K_R \rangle}, \quad (8)$$

where  $\bar{K}_R$  denotes the nonequilibrium ensemble average of the rotational kinetic energy of the central excited molecule, and  $\langle K_R \rangle$  its equilibrium average value, the excess rotational kinetic energy function plotted in Fig. 2.

In the equilibrium case, the rotational energy fluctuations are conveniently characterized by the normalized equilibrium time correlation function

$$C_R(t) = \frac{\langle \delta K_R(t) \delta K_R(0) \rangle}{\langle \delta K_R(0) \delta K_R(0) \rangle}, \quad (9)$$

with the brackets indicating an equilibrium average and  $\delta K_R(t) = K_R(t) - \langle K_R \rangle$  denoting the fluctuations about the equilibrium average  $\langle K_R \rangle$ . In the linear response regime, the response function and the TCF are equal.

The LRT assumption is assessed in Fig. 4, which compares, for all four liquids, the time evolution of  $C_R$  with that of  $S_R$  for several initial rotational energy excitation values (the H-bond liquid nonequilibrium results are based on  $x$ -axis excitation). For each liquid, LRT is quite accurate for the 1 kcal/mol excitation case, i.e. just outside the thermal range:  $S_R$  and  $C_R$  are almost identical for all liquids. But as the excitation energy is increased, the response function progressively deviates from the TCF to varying degrees for the different liquids.

We focus first on the H-bonded liquids. At the 5 kcal/mol level of excitation, LRT continues to hold well for H<sub>2</sub>O, but starts to noticeably degrade for the more weakly H-bonded MeOH as its oscillations are delayed and suppressed past the second minimum. Increasing the excitation to 15 kcal/mol leaves only one smallish amplitude libration evident, a feature shared with H<sub>2</sub>O for which difficulties with LRT are now evident.

The increasing deterioration of LRT's validity with the larger initial rotational excitation also occurs for the non-polar liquids CCl<sub>4</sub> and CH<sub>4</sub>, with the trend of slowing of

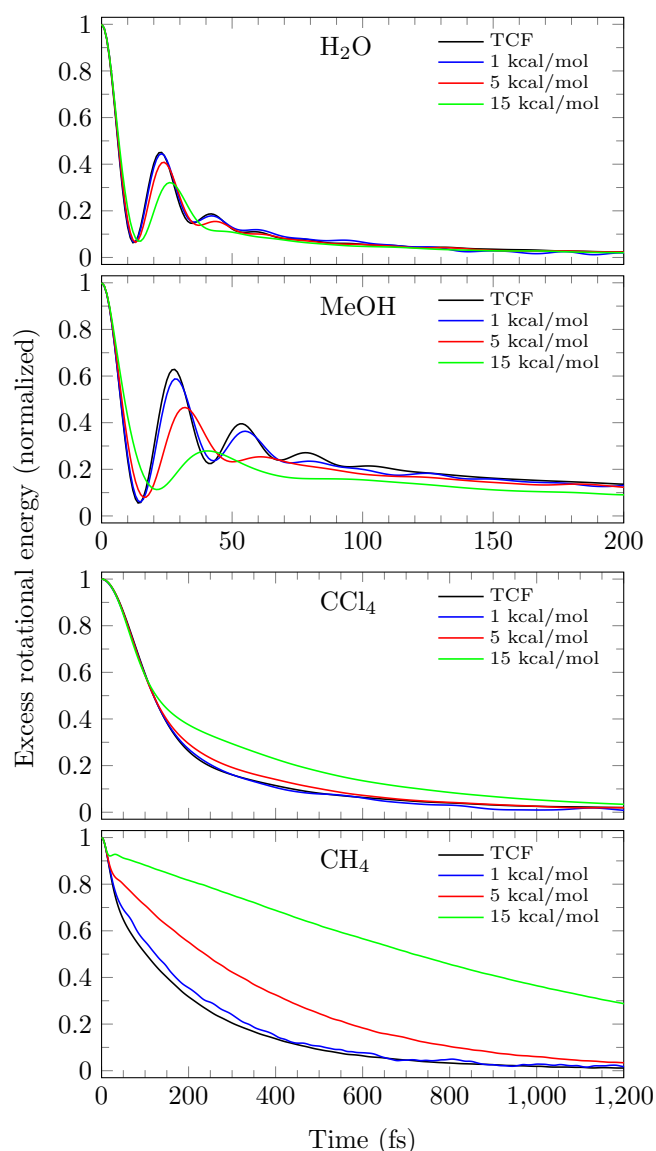


FIG. 4: Test of Linear Response Theory (LRT) for the four liquids, and for three different rotational energy excitation values. For each liquid, the equilibrium TCF  $C(t)$  Eq. 9 is compared, versus time, with the nonequilibrium relaxation function  $S_R(t)$ , Eq. 8, reflecting the normalized excess rotational kinetic energy subsequent to the central molecule  $C$ 's instantaneous rotational excitation with respect to the principal  $x$ -axis. Note the time axis change in the panels for the nonpolar liquids compared to the H-bond liquids. Additional results are given in SI Sec. S3.

the relaxation more evident—especially for CH<sub>4</sub>—than for the H-bonded liquids' oscillation-dominated appearance. Indeed, this slowing in the mainly nonoscillatory "tails" of the nonequilibrium  $S_R(t)$  is only marked for CH<sub>4</sub>. For this liquid, the relaxation time (defined as the integral of the normalized TCF) slows by about a factor of 4 at the highest excitation energy.

When the excitation energy is increased to

15 kcal/mol, the H<sub>2</sub>O and CCl<sub>4</sub> response functions show significant deviations from the corresponding TCFs. Nonetheless, the time of complete relaxation is not greatly affected for these two liquids; this is also observed for MeOH, but not for CH<sub>4</sub>, as noted above. In fact, this CH<sub>4</sub>  $S_R - C_R$  disparity is very similar to the nonlinear response observed for solute rotation in Ref. 30. There linear response broke down shortly after excitation, with subsequent relaxation significantly slowed. The short period of time for which  $S_R$  followed  $C_R$  roughly equaled one quarter of the free rotational period  $\sim 135$  fs for the specific excitation energy.<sup>30</sup> For comparison, for CH<sub>4</sub> (in CH<sub>4</sub>) the onset of nonlinear response occurs at  $t \approx 20$  fs, which is  $\sim 1/7$  of the 15 kcal/mol excitation rotational period. Now pursuing this nonlinear response onset aspect, a distinct local maximum in  $S_R$  is observed as well in CCl<sub>4</sub>, but at the higher threshold energy  $\sim 70$  kcal/mol (See Fig. S3.1). Here, the onset occurs at  $t \approx 80$  fs, which is  $\sim 1/8$  of the rotational period  $\sim 630$  fs for 70 kcal/mol excitation. The highest excitation results in Fig. S3.1 for the spherical top molecules strongly suggest nearly free rotation. Indeed, for the nonpolar molecules—especially the nearly spherical CH<sub>4</sub>—the increasing dominance of the excitation kinetic energy over the weak intermolecular angular interactions provides the basic rationale for the increasingly slow relaxation time behavior.

Returning to a focus on the H-bonded liquids, even though linear response theory breaks down for them when the rotational excitation energy exceeds  $\sim 5$ –15 kcal/mol (see also Fig. S3.1), it is important to note that the “long” time behavior of the normalized response function is almost independent of the excitation energy, i.e., the percentage loss of excess energy after  $\sim 100$  fs is nearly invariant to the strength of the perturbation, and no indication of free rotation is evident.

For all of these excitation cases, we have computed the work terms for rotation and translation, and their first solvent shell analogues. For both of the nonpolar solvents CCl<sub>4</sub> and CH<sub>4</sub>, the increase in excitation energy does not change the asymptotic values of the work terms in any significant way; and likewise the locality of the relaxation process seems largely unchanged, see SI. The latter observation might be expected, since here we determine locality based on the four closest neighbors, and not a distance criterion<sup>22,23</sup> which could reveal e.g. any expansion of the first shell at the onset of nonlinear response. In contrast, for H<sub>2</sub>O and MeOH the work terms are somewhat dependent on the excitation energy for  $x$ -axis excitation, see SI. The variation of the work for these H-bonded liquids shows that the energy transfer efficiency to the solvent molecules’ rotational modes decreases with increasing excitation energy: the drop is  $\sim 10$  % for H<sub>2</sub>O and  $\sim 20$  % for MeOH for the energy range 1 – 30 kcal/mol. This decrease in the  $W_R$  fractional contribution is obviously compensated by an equal increase in the percentage contribution of the energy flow  $W_T$  to the solvent molecules’ translational motions. These features likely reflect the

decreasing relevance of torques in the face of increasing excitation, with lower susceptibility for the stronger water interactions. These variations have a locality aspect: we observe that the increased transfer to translational modes takes place almost entirely within the first solvent shell for both liquids. But the decreasing relative contribution of the rotational energy flow  $W_R$  has a more intriguing behavior: for water, it is mostly due to a less efficient transfer to neighbors outside the first shell, but for methanol the opposite scenario holds, with a less efficient transfer to neighbors inside the first shell.

## B. Translational energy relaxation

We have seen in Sec. IV A that, for the case of initial rotational energy excitation, the energy transfer between rotational and translational motions is very important for the nonpolar liquids CCl<sub>4</sub> and CH<sub>4</sub> and, although smaller, is non-negligible for H<sub>2</sub>O and MeOH H-bonded liquids. In this section, we make a comparative investigation of the relaxation and energy flow pathways for an initial translational energy excitation.

We commence with the excess translational kinetic energy ( $\delta K_T$ ) of the central excited molecule C, normalized to its initial excitation value, as a function of time for a slightly suprathreshold 1 kcal/mol excitation, see Fig. 5. The ultrafast translational energy decay proceeds monotonically for all four neat liquids, at least initially, with very subdued oscillations subsequently apparent for the H-bonded liquids; these are not dissimilar, though delayed in time, to the features seen for these liquids after rotational excitation in Fig. 2. In particular, and unsurprisingly, the decay is fastest in the H-bonded liquids, as it was for the rotational energy relaxation.

### 1. Energy flow and work.

In Section IV A 1, we found that the transfer efficiency of the excess rotational kinetic energy to translational and rotational modes of the solvent displayed a different character for the H-bonded liquids and the nonpolar liquids. Is a similar behavior exhibited for translational energy relaxation? For this purpose, the time evolution of the energy and work terms in Eq. (6) are shown in Fig. 6 up through the first 500 fs after instantaneous 5 kcal/mol translational excitation of the central molecule.

Fig. 6 shows that, in analogy to the rotational relaxation case, the initial increase in  $|\Delta K_{T,C}|$  (i.e., the decrease in C’s translational energy) is initially strongly correlated with an increase in the intermolecular potential energy term  $\Delta U$ . But further examination reveals that the different behavior, especially for energy transfer efficiency, between H-bonded liquids and the nonpolar liquids observed for rotational energy relaxation is not repeated for translational energy relaxation. First, for the decay, while the H-bonded liquids have the fastest decay,

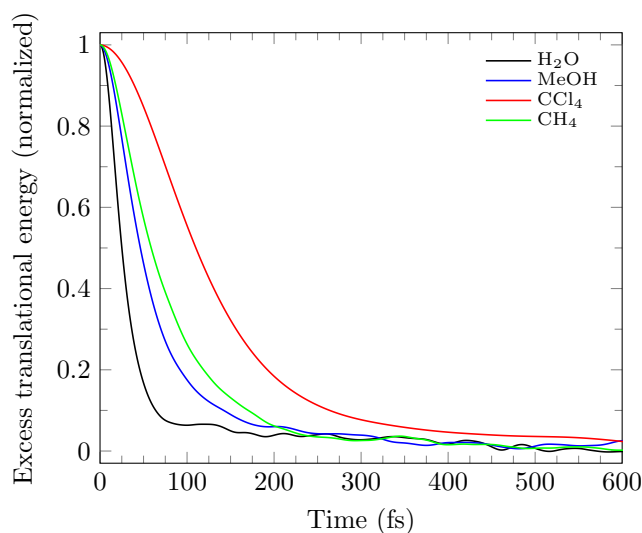


FIG. 5: Normalized (to the initial excitation value) excess translational kinetic energy of a central molecule C as a function of time subsequent to a 1 kcal/mol translational kinetic energy excitation of a central molecule C in each of the four liquids.

TABLE III: Normalized work terms  $W_T$  (energy flow to translation) and  $W_R$  (energy flow to rotation) after 5 ps following 5 kcal/mol translational excitation. For the final two columns, the 1st solvent shell is defined as the four nearest molecules (see the text).

	Solvent		1st solvent shell	
	$W_T$ (%)	$W_R$ (%)	$W_T$ (%)	$W_R$ (%)
H <sub>2</sub> O	76	22	73	20
MeOH	59	39	53	35
CCl <sub>4</sub>	63	35	62	34
CH <sub>4</sub>	76	22	74	21

here methane is essentially as fast as methanol, presumably due to the former's smallest mass among the four liquids. Second, for the transfer efficiency, this is quantified by the work terms, which depart from the rotational excitation behavior. After a short delay, the work terms  $W_T$  and  $W_R$  monitoring energy flow each start to build up, with transfer to the surrounding "solvent"'s translational moment clearly dominant for all liquids. The efficiency of this flow, given in Table III at 5 ps, is largest, not for the two H-bonded liquids, but instead for the two lightest molecules in this study, water and methane: their  $W_T$  values are identical, evidently another appearance of the importance of mass for the translational energy transfer. Indeed—and quite surprisingly—the similarity in the work terms is sorted, not by H-bonded vs non-polar liquids as it was for rotational excitation, but by two molecular pairs H<sub>2</sub>O/CH<sub>4</sub> and MeOH/CCl<sub>4</sub>, with the two members of each pair being extremely close to each other (identical for the first pair).

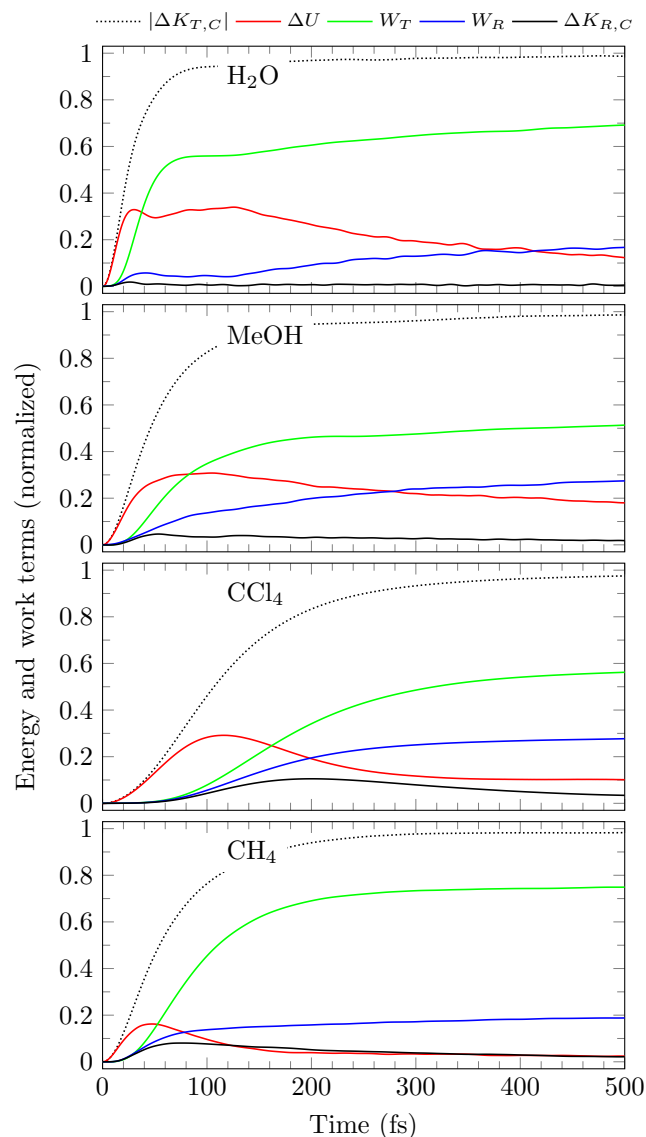


FIG. 6: Normalized (to the initial excitation kinetic energy) kinetic energy, potential energy and work terms (the latter gauging energy flow to the solvent translational (T) and rotational (R) motions) for the excited central molecule C's translational energy relaxation in the four liquids following its instantaneous 5 kcal/mol excitation. Black dotted: change in central molecule translational kinetic energy  $\Delta K_{T,C}$ ; red: potential energy change  $\Delta U$ ; green: translational work  $W_T$ ; blue: rotational work  $W_R$ ; black solid: change in C's rotational kinetic energy  $|\Delta K_{R,C}|$ . Further Work results are given in SI Sec. S2.

## 2. Locality of relaxation process.

Again, we exploit the work/power formalism, and determine the locality of the energy flow process—now from the translationally excited C molecule—in terms of the transferred energy to the first solvent shell neighbors (we retain the 1st shell definitions as consisting of the four

nearest neighbors). The asymptotic values of  $W_T$  and  $W_R$  for energy flows to solvent translational and rotational motions respectively for the first solvent shell, at  $t = 5$  ps, are shown in the last two columns of Table III. Clearly there is little delocalization of the energy flow from the translationally excited C for any of the liquids. In particular, while the flow for  $\text{CCl}_4$  and  $\text{CH}_4$  is localized, the observed delocalization extent for the rotational excitation case in  $\text{H}_2\text{O}$  and  $\text{MeOH}$  in Table III is greatly diminished here: only  $\sim 5 - 10\%$  of C's excess translational kinetic energy is transferred to neighbors outside the first solvent shell. Presumably this restricted extent feature reflects the lack of importance for translation, in contrast to the rotational case, of longer-range dipole-dipole interactions.

### 3. Linear response regime.

Lastly, we investigate how well linear response theory describes translational energy relaxation. In Fig. 7, the time evolution of the response function for the nonequilibrium translational kinetic energy, for different excitation energies, and the TCF for equilibrium fluctuations of the translational kinetic energy are shown. As opposed to the rotational relaxation case, linear response theory seems to be applicable up to, at least,  $\sim 5$  kcal/mol translational excitation energy for all liquids. Only in the case of  $\text{CCl}_4$  and  $\text{CH}_4$ , does the response function deviate significantly from the TCF as the translational excitation energy is increased further. For  $\text{H}_2\text{O}$  and  $\text{MeOH}$ , no significant breakdown of linear response is observed, even for an excitation energy of  $60$  kcal/mol  $\approx 100 k_B T$  (see Fig. S3.2). Finally, for the nonpolar liquids, the translational relaxation accelerates in Fig. 7 with increasing translation excitation energy, in contrast with the slowing exhibited in Fig. 4 for the rotational case. As we noted in connection with the latter, the weak intermolecular interactions are the source of the observed rotational behavior. But for translation, stronger interactions via collisions are essentially guaranteed with increasing translational excitation energy, and the relaxation is accelerated.

For all four liquids, the transfer efficiency to translational modes increases slightly with increasing excitation energy, see SI Sec. S2. For  $\text{MeOH}$  and  $\text{CCl}_4$ , an increase of  $\sim 10\%$  — for the excitation energy range of  $1 - 60$  kcal/mol — is observed, whereas the increase is only a few percent for  $\text{H}_2\text{O}$  and  $\text{CH}_4$ . In general the translational relaxation process becomes slightly more local with increasing excitation energy, with a small increase in the transfer efficiency to the translational modes of the first solvent shell molecules.

## V. CONCLUDING REMARKS

We have investigated ultrafast rotational and translational energy relaxation for intramural excitation of a

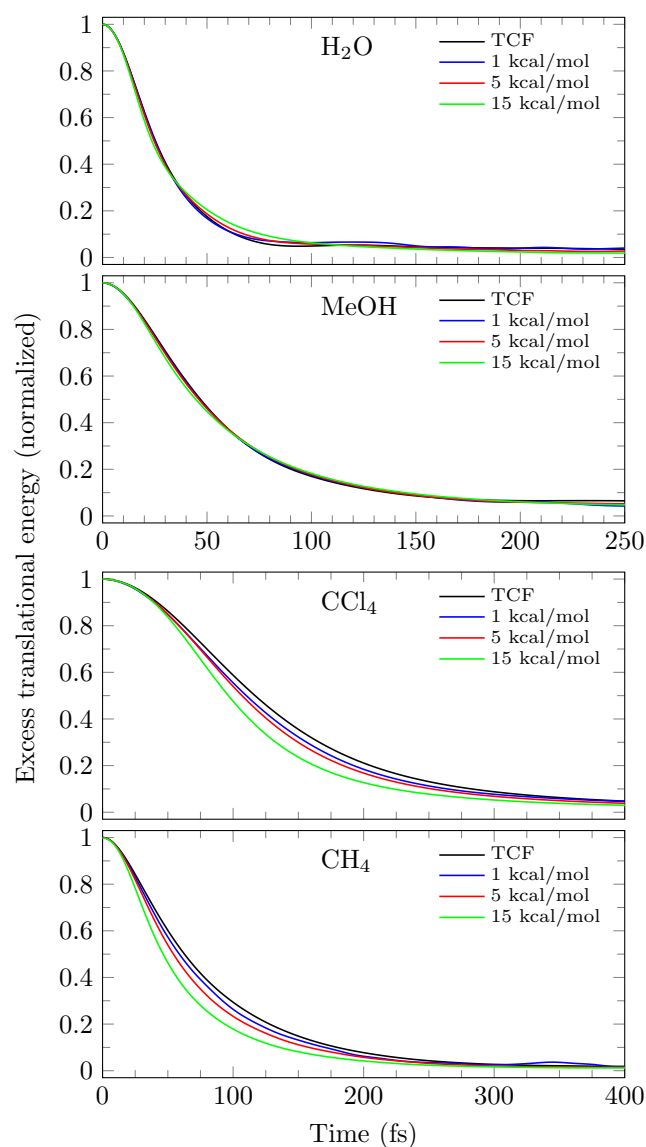


FIG. 7: Normalized excess translational kinetic energy—the translational analogue of Eq. 8—as a function of time subsequent to instantaneous translational excitation. Note the change of the time axis in the panels showing results for  $\text{CCl}_4$  and  $\text{CH}_4$ . These and further excitation energy results are used in SI Fig. S3.2 to examine the validity of linear response theory (LRT) for the translational case.

molecule in each one of four neat liquids—the two H-bonded liquids  $\text{H}_2\text{O}$  and  $\text{MeOH}$ —and the two nonpolar liquids  $\text{CCl}_4$  and  $\text{CH}_4$ , e.g. excitation of an  $\text{H}_2\text{O}$  molecule “solute” in liquid  $\text{H}_2\text{O}$  “solvent”. To this end, we have employed nonequilibrium and equilibrium classical molecular dynamics simulations and energy flux analysis, which allows a detailed identification of the energy flow pathways during relaxation. As stressed in the Introduction, these studies should prove relevant for modern ultrafast terahertz and x-ray experiments as well as for novel phenomena such as self-thermophoresis. Further,

1 some of the excitations considered, in the text and in  
2 SI, involve energies of magnitude associated with highly  
3 exothermic chemical processes, see e.g. Ref. 42–44. Here  
4 we briefly summarize the main conclusions, beginning  
5 with the rotational excitation results.

6 Relaxation dynamics for rotational excitation is ultra-  
7 fast, i.e., the energy dissipation is completed within 1 ps,  
8 and is significantly faster for H<sub>2</sub>O and MeOH. Partial  
9 coherence—due to OH librational motions—occurs for  
10 the H-bonded liquids, but monotonic decay character-  
11 izes the nonpolar liquids. Most of the excess rotational  
12 kinetic energy is transferred to librational motions for  
13 the H-bonded liquids (although this flow direction dom-  
14 inance decreases with increasing excitation energy). In  
15 contrast, transfer efficiencies to translational and rota-  
16 tional motions are nearly equal for the nonpolar liquids.  
17 Almost all of this excess energy is transferred to first sol-  
18 vent shell neighbors for CCl<sub>4</sub> and CH<sub>4</sub>, but the flow is  
19 less local for MeOH and H<sub>2</sub>O: 15–23 % and 18–28 % of  
20 the energy (depending on the excitation axis) is trans-  
21 ferred to neighbors beyond the first shell, respectively.  
22 Finally, linear response theory (LRT) is applicable for all  
23 four liquids for 1 kcal/mol excitations. For the excitation  
24 levels examined the threshold energy at the nonlinear re-  
25 sponse onset is ~5 kcal/mol for MeOH and CH<sub>4</sub>, and  
26 ~15 kcal/mol for H<sub>2</sub>O and CCl<sub>4</sub>.

27 The translational energy excitation results often dif-  
28 fer, sometimes very considerably, from those following  
29 rotational excitation. The relaxation is ultrafast, but the  
30 excess translational kinetic energy decays monotonically,  
31 without any evidence for coherence, for all four liquids  
32 (there is some flow to the H-bonded “solvent” librations,  
33 but it is evidently incoherent). Again, the relaxation is  
34 significantly faster for H<sub>2</sub>O and MeOH, but transfer to  
35 the “solvent” molecules’ translational motions dominates  
36 for all four liquids, most especially for the lighter H<sub>2</sub>O  
37 and CH<sub>4</sub>. (The efficiencies of the transfer of excess en-  
38 ergy to translational and rotational motions now depend  
39 only weakly on the excitation energy.) The energy flow  
40 is again local for the non-polar liquids, but is now more  
41 local for the H-bonded liquids than for the rotational ex-  
42 citation case. Finally, LRT is considerably more resilient  
43 than for rotational excitation, with onset of significant  
44 nonlinear response only observed for the nonpolar liq-  
45 uids, and then only for excitations of tens of kcal/mol  
(See SI Sec. S3).

46 As noted within, the work/power formulation for en-  
47 ergy flow has not been fully exploited in the current  
48 effort, devoted to the comparison between examples of

hydrogen-bonded and non-polar solvents. More can be  
done for these solvents, solvent classes,<sup>3,20–23</sup> as well as  
mixed solutions; clearly polar non-hydroxylic solvents  
such as acetonitrile (see e.g. Ref. 72) merit compara-  
ble attention in the future as well. As for the present  
liquids—most especially water for which most experi-  
ments referred to in the Introduction have been carried  
out—extension of the energy flow formulation to e.g. spe-  
cific spatial and structural variables directly related to  
measured spectra (e.g. transition dipole orientational an-  
gles as in Ref. 11) or configurational variables (e.g. as  
probed in the x-ray studies of Ref. 72) could be carried  
out in the future in direct connection with the present  
kinetic energy studies. Indeed, we have previously exam-  
ined the dynamics of such variables previously for pure  
water (e.g. Refs. 19–23). Such “double variable” studies  
could relate the time scales found here and those associ-  
ated with e.g. reorientation in Ref. 11 and solvent cage  
rearrangement in Ref. 72. Returning to the kinetic en-  
ergy arena, a further application of the energy flow for-  
malism could be to the examination of the participation  
of assorted modes of liquid motion in the energy relax-  
ation, where resonance and coupling issues will be cru-  
cial (e.g. Refs. 17,18,24) and features such as transient  
or complete rupture of hydrogen bonds.<sup>73–76</sup> More gen-  
erally, these several avenues would also serve to provide  
a detailed molecular level mechanism, both kinetic and  
configurational, for the energy flow.

### Acknowledgments

This work was supported by MICINN grant PGC2018-099277-B-C21 (RR), and NSF grant CHE-1112564 (JTH). JP and KBM were supported by the Danish National Research Foundation.

### Supplementary Information

There are three Supplementary Information sections: Supplementary Information, Rotational Excitation: Rotational and Translational Work for the Four Liquids, Translational Excitation: Translational and Rotation Work for the Four Liquids, and Tests of Linear Response Theory for Rotational and Translational Excitations for the Four Liquids.

### REFERENCES

- 1 Cho, M.; Fleming, G.R. Electron Transfer and Solvent Dynamics in Two- and Three-State Systems. *Adv. Chem. Phys.* **1999**, *107*, 311–370.
- 2 Bagchi, B.; Jana, B. Solvation Dynamics in Dipolar Liq-

\* Electronic address: [petersen.jakob@icloud.com](mailto:petersen.jakob@icloud.com)

† Electronic address: [kbmo@kemi.dtu.dk](mailto:kbmo@kemi.dtu.dk)

‡ Electronic address: [james.hynes@colorado.edu](mailto:james.hynes@colorado.edu)

§ Electronic address: [rosendo.rey@upc.edu](mailto:rosendo.rey@upc.edu)

- uids. *Chem. Soc. Rev.* **2010**, *39*, 1936-1954.
- <sup>3</sup> Rey, R.; Hynes, J.T. Solvation Dynamics in Water. 4. On the Initial Regime of Solvation Relaxation. *J. Phys. Chem. B* **2020**, *124*, 7668-7681.
- <sup>4</sup> Rey, R.; Møller, K.B.; Hynes, J.T. Ultrafast Vibrational Population Dynamics of Water and Related Systems : A Theoretical Perspective. *Chem. Rev.* **2004**, *104*, 1915-1928.
- <sup>5</sup> Yu, C.C.; Chiang, K.Y.; Okuno, M.; Seki, T.; Ohto, T.; Yu, X.; Korepanov, V.; Hamaguchi, H.O.; Bonn, M.; Hunger, J. et al. Vibrational Couplings and Energy Transfer Pathways of Water's Bending Mode. *Nat. Comm.* **2020**, *11*, 5977.
- <sup>6</sup> Baiz, C.R.; Blasiak, B.; Bredenbeck, J.; Cho, M.; Choi, J.H.; Corcelli, S.A.; Dijkstra, A.G.; Feng, C.J.; Garrett-Roe, S.; Ge, N.H. et al. Vibrational Spectroscopic Map, Vibrational Spectroscopy, and Intermolecular Interaction. *Chem. Rev.* **2020**, *120*, 7152-7218.
- <sup>7</sup> Elgabarty, H.; Kampfrath, T.; Bonthuis, D. J.; Balos, V.; Kaliannan, N. K.; Loche, P.; Netz, R. R.; Wolf, M.; Kühne, T. D.; Sajadi, M. Energy Transfer Within the Hydrogen Bonding Network of Water Following Resonant Terahertz Excitation. *Sci. Adv.* **2020**, *6*, eaay7074.
- <sup>8</sup> Zhao, H.; Tan, Y.; Zhang, L.; Zhang, R.; Shalaby, M.; Zhang, C.; Zhao, Y.; Zhang, X.C. Ultrafast Hydrogen Bond Dynamics of Liquid Water Revealed by Terahertz-Induced Transient Birefringence. *Light Sci. Appl.* **2020**, *9*, 136.
- <sup>9</sup> Kim, K. H.; Spah, A.; Pathak, H.; Yang, C.; Bonetti, S.; Amann-Winkel, K.; Mariedahl, D.; Schlesinger, D.; Sellberg, J. A.; Mendez, D. et al. Anisotropic X-Ray Scattering of Transiently Oriented Water. *Phys. Rev. Lett.*, **2020**, *125*, 076002.
- <sup>10</sup> Perakis, F.; Camisasca, G.; Lane, T.J.; Spah, A.; Wikfeldt, K.T.; Sellberg, J.A.; Lehmkuhler, F.; Pathak, H.; Kim, K.H.; Amann-Winkel, K. et al. Coherent X-rays Reveal the Influence of Cage Effects on Ultrafast Water Dynamics. *Nat. Comm.* **2018**, *9*, 1917.
- <sup>11</sup> Novelli, F.; Ruiz Pestana, L.; Bennett, K.C.; Sebastiani, F.; Adams, E.M.; Stavrias, N.; Ockelmann, T.; Colchero, A.; Hoberg, C.; Schwaab, G. et al. Strong Anisotropy in Liquid Water upon Librational Excitation Using Terahertz Laser Fields. *J. Phys. Chem. B* **2020**, *124*, 4989-5001.
- <sup>12</sup> van Driel, T.B.; Kjaer, K.S.; Hartsock, R.W.; Dohn, A.O.; Harlang, T.; Chollet, M.; Christensen, M.; Gawelda, W.; Henriksen, N.E.; Kim, J.G. et al. Atomistic Characterization of the Active-Site Solvation Dynamics of a Model Photocatalyst. *Nat. Comm.* **2016**, *7*, 13678.
- <sup>13</sup> Biasin, E.; Fox, Z.W.; Andersen, A.; Ledbetter, K.; Kjaer, K.S.; Alonso-Mori, R.; Carlstad, J.M.; Chollet, M.; Gaynor, J.D.; Glownia, J.M. et al. Direct Observation of Coherent Femtosecond Solvent Reorganization Coupled to Intramolecular Electron Transfer. *Nat. Chem.* **2021**, *13*, 343-349.
- <sup>14</sup> Calero, C.; Sibert, E.L.; Rey, R. Self-Thermophoresis at the Nanoscale Using Light Induced Solvation Dynamics. *Nanoscale* **2020**, *12*, 7557-7562.
- <sup>15</sup> Whitnell, R.M.; Wilson, K.R.; Hynes, J.T. Vibrational Relaxation of a Dipolar Molecule in Water. *J. Chem. Phys.* **1992**, *96*, 5354-5369.
- <sup>16</sup> Gertner, B.J.; Whitnell, R.M.; Wilson, K.R.; Hynes, J.T. Activation to the Transition State: Reactant and Solvent Energy Flow for a Model SN2 Reaction in Water. *J. Amer. Chem. Soc.* **1991**, *113*, 74-87.
- <sup>17</sup> Rey, R.; Hynes, J.T. Tracking Energy Transfer from Excited to Accepting Modes: Application to Water Bend Vibrational Relaxation. *Phys. Chem. Chem. Phys.* **2012**, *14*, 6332-6342.
- <sup>18</sup> Rey, R.; Ingrosso, F.; Elsaesser, T.; Hynes, J.T. Pathways for H<sub>2</sub>O Bend Vibrational Relaxation in Liquid Water. *J. Phys. Chem. A* **2009**, *113*, 8949-8962.
- <sup>19</sup> Petersen, J.; Møller, K.B.; Rey, R.; Hynes, J.T. Ultrafast Librational Relaxation of H<sub>2</sub>O in Liquid Water. *J. Phys. Chem. B* **2013**, *117*, 4541-4552.
- <sup>20</sup> Rey, R.; Hynes, J.T. Solvation dynamics in liquid water. I. Ultrafast energy fluxes. *J. Phys. Chem. B*, **2015**, *119*, 7558-7570.
- <sup>21</sup> Rey, R.; Hynes, J.T. Solvation Dynamics in Water: 2. Energy Fluxes on Excited- and Ground-State Surfaces. *J. Phys. Chem. B* **2016**, *120*, 11287-11297.
- <sup>22</sup> Rey, R.; Hynes, J.T. Solvation Dynamics in Liquid Water. III. Energy Fluxes and Structural Changes. *J. Phys. Chem. B* **2017**, *121*, 1377-1385.
- <sup>23</sup> Rey, R.; Hynes, J.T. Translational versus rotational energy flow in water solvation dynamics. *Chem. Phys. Lett.* **2017**, *683*, 483-487.
- <sup>24</sup> Kandratsenka, A.; Schroeder, J.; Schwarzer, D.; Vikhrenko, V. S. Nonequilibrium molecular dynamics simulations of vibrational energy relaxation of HOD in D<sub>2</sub>O. *J. Chem. Phys.* **2009**, *130*, 174507.
- <sup>25</sup> Vikhrenko, V. S.; Heidelberg, C.; Schwarzer, D.; Nemtsov, V. B.; Schroeder, J. Molecular dynamics simulation of vibrational energy relaxation of highly excited molecules in fluids. I. General considerations. *J. Chem. Phys.* **1999**, *110*, 5273-5285.
- <sup>26</sup> Heidelberg, C.; Vikhrenko, V. S.; Schwarzer, D.; Schroeder, J. Molecular dynamics simulation of vibrational relaxation of highly excited molecules in fluids. II. Nonequilibrium simulation of azulene in CO<sub>2</sub> and Xe. *J. Chem. Phys.* **1999**, *110*, 5286-5299.
- <sup>27</sup> Heidelberg, C.; Schroeder, J.; Schwarzer, D.; Vikhrenko, V. S., Mode specificity of vibrational energy relaxation of azulene in CO<sub>2</sub> at low and high density. *Chem. Phys. Lett.* **1998**, *291*, 333-340.
- <sup>28</sup> Tao, G.; Stratt, R.M. Anomalously Slow Solvent Structural Relaxation Accompanying High-Energy Rotational Relaxation. *J. Phys. Chem. B* **2008**, *112*, 369-377.
- <sup>29</sup> Tao, G.; Stratt, R.M. The Molecular Origins of Nonlinear Response in Solute Energy Relaxation: The Example of High-Energy Rotational Relaxation. *J. Chem. Phys.* **2006**, *125*, 114501.
- <sup>30</sup> Moskun, A.C.; Jailaubekov, A.E.; Bradforth, S.E.; Tao, G.; Stratt, R.M. Rotational Coherence and a Sudden Breakdown in Linear Response Seen in Room-Temperature Liquids. *Science* **2006**, *311*, 1907-1911.
- <sup>31</sup> Yagasaki, T.; Saito, S. A novel method for analyzing energy relaxation in condensed phases using nonequilibrium molecular dynamics simulations: Application to the energy relaxation of intermolecular motions in liquid water. *J. Chem. Phys.* **2011**, *134*, 184503.
- <sup>32</sup> Evans, M.W.; Ferrario, M. The correlation of molecular rotational and translational kinetic energy in liquid CH<sub>2</sub>Cl<sub>2</sub> and CHCl<sub>3</sub>. *Advances in Molecular Relaxation and Interaction Processes* **1982**, *23*, 69-73.
- <sup>33</sup> Padró, J. A.; Trullàs, J.; Sesé, G. Computer simulation study of the dynamic cross-correlations in liquids. *Mol. Phys.* **1991**, *72*, 1035-1049.
- <sup>34</sup> Balucani, U.; Vallauri, R.; Gaskell, T.; Gori, M. Microscopic dynamics in liquid rubidium. *Phys. Lett. A* **1984**,

- 102, 109-114.
- 35 Yardley, J. T. Introduction to Molecular Energy Transfer. Academic Press, 1980.
- 36 Jang, J.; Stratt, R. M. Dephasing of individual rotational states in liquids. *J. Chem. Phys.* **2000**, *113* 11212-11221.
- 37 Laage, D. Reinterpretation of the Liquid Water Quasi-Elastic Neutron Scattering Spectra Based on a Nondiffusive Jump Reorientation Mechanism. *J. Phys. Chem. B* **2009**, *113*, 2684-2687.
- 38 Hardy, E. H.; Zygar, A.; Zeidler, M. D.; Holz, M.; Sacher, F. D. Isotope Effect on the Translational and Rotational Motion in Liquid Water and Ammonia. *J. Chem. Phys.* **2001**, *114*, 3174-3181.
- 39 Holz, M.; Mao, X.-A.; Seiferling, D.; Sacco, A. Experimental Study of Dynamic Isotope Effects in Molecular Liquids: Detection of Translation-Rotation Coupling. *J. Chem. Phys.* **1996**, *104*, 669-679.
- 40 Buchhauser, J.; Groß, T.; Karger, N.; Lüdemann, H.-D. Self-diffusion in CD<sub>4</sub> and ND<sub>3</sub>: with Notes on the Dynamic Isotope Effect in Liquids. *J. Chem. Phys.* **1999**, *110*, 3037-3042.
- 41 Ingrosso, F.; Rey, R.; Elsaesser, T.; Hynes, J.T. Ultrafast Energy Transfer from the Intramolecular Bending Vibration to Librations in Liquid Water. *J. Phys. Chem. A* **2009**, *113*, 6657-6665.
- 42 Grubb, M.P.; Coulter, P.M.; Marroux, H.J.B.; Hornung, B.; McMullen, R.S.; Orr-Ewing, A.J.; Ashfold, M.N.R. Translational, Rotational and Vibrational Relaxation Dynamics of a Solute Molecule in a Non-Interacting Solvent. *Nat. Chem.* **2016**, *8*, 1042-1046.
- 43 Murray, M.J.; Ogden, H.M.; Toro, C.; Liu, Q.; Mullin, A.S. Impulsive Collision Dynamics of CO Super Rotors from an Optical Centrifuge. *ChemPhysChem* **2016**, *17*, 3692-2700.
- 44 Michael, T.J.; Ogden, H.M.; Mullin, A.S. State-resolved rotational distributions and collision dynamics of CO molecules made in a tunable optical centrifuge. *J. Chem. Phys.* **2021**, *154*, 134307.
- 45 Matsumoto, M.; Gubbins, K.E. Hydrogen bonding in liquid methanol. *J. Chem. Phys.* **1990**, *93*, 1981-1994.
- 46 Pagitsas, M.; Hynes, J.T.; Kapral, R. Kinetic Energy Relaxation of a Test Particle in a Dense Fluid. *J. Chem. Phys.* **1979**, *71*, 4492-4501.
- 47 Rey, R.; Hynes, J.T. Vibrational Relaxation of HOD in D<sub>2</sub>O. *J. Chem. Phys.* **1996**, *104*, 2356-2368.
- 48 Tran, V.; Schwartz, B.J. Role of Nonpolar Forces in Aqueous Solvation: Computer Simulation Study of Solvation Dynamics in Water Following Changes in Solute Size, Shape and Charge. *J. Phys. Chem. B* **1999**, *103*, 5570-5580.
- 49 Fonseca, T.; Ladanyi, B.M. Breakdown of Linear Response for Solvation Dynamics in Methanol. *J. Phys. Chem.* **1991**, *95*, 2116-2119.
- 50 Carter, E.; Hynes, J.T. Solvation Dynamics for an Ion Pair in a Polar Solvent: Time-Dependent Fluorescence and Photochemical Charge Transfer. *J. Chem. Phys.* **1991**, *94*, 5961-5979.
- 51 Maroncelli, M.; Fleming, G.R. Computer Simulation of the Dynamics of Aqueous Solvation. *J. Chem. Phys.* **1988**, *89*, 5044-5068.
- 52 Andersen, H. C. RATTLE A Velocity Version of the Shake Algorithm for Molecular-Dynamics Calculations. *J. Comput. Phys.* **1983**, *52*, 24-34.
- 53 Hoover, W. G. Canonical Dynamics - Equilibrium Phase-Space Distributions. *Phys. Rev. A* **1985**, *31*, 1695-1697.
- 54 Nosé, S. A Molecular-Dynamics Method for Simulations in the Canonical Ensemble. *Mol. Phys.* **1984**, *52*, 255-268.
- 55 Berendsen, H. J. C.; Grigera, J. R.; Straatsma, T. P. The Missing Term in Effective Pair Potentials. *J. Phys. Chem.* **1987**, *91*, 6269-6271.
- 56 Jorgensen, W. L. Optimized Intermolecular Potential Functions for Liquid Alcohols. *J. Phys. Chem.* **1986**, *90*, 1276-1284.
- 57 Skarmoutsos, I.; Kampanakis, L. I.; Samios, J. Investigation of the vapor-liquid equilibrium and supercritical phase of pure methane via computer simulations. *J. Mol. Liq.* **2005**, *117*, 33-41.
- 58 Rey, R.; Pardo, L. C.; Llanta, E.; Ando, K.; López, D. O.; Tamari, J. Ll. and Barrio, M. X-ray and molecular dynamics study of liquid structure in pure methylchloromethane compounds ( (CH<sub>3</sub>)<sub>4</sub>nCCln). *J. Chem. Phys.* **2000**, *112*, 7505-7517.
- 59 Garberoglio, G.; Paqualini, F.; Sutmann, G.; Vallauri, R. Dynamical Properties of Hydrogen Bonded Liquids. *J. Mol. Liq.* **2002**, *96-7*, 19-29.
- 60 Rosenthal, S.J.; Jimenez, R.; Fleming, G.R.; Kumar, P.V.; Maroncelli, M. Solvation Dynamics in Methanol: Experimental and Molecular Dynamics Simulation Studies *J. Mol. Liq.* **1994**, *60*, 25-56.
- 61 Bako, I.; Bencsura, A.; Hermansson, K.; Balint, S.; Grosz, T.; Chihai, V.; Olah, J. Hydrogen Bond Network Topology in Liquid Water and Methanol: a Graph Theory Approach. *Phys. Chem. Chem. Phys.* **2013**, *15*, 151630.
- 62 Haughney, M.; Ferrario, M.; McDonald, I. R. Molecular-Dynamics Simulation of Liquid Methanol. *J. Phys. Chem.* **1987**, *91*, 4934-4940.
- 63 Rey, R. Is There a Common Orientational Order for the Liquid Phase of Tetrahedral Molecules? *J. Chem. Phys.* **2009**, *131*, 064502.
- 64 Rey, R. Quantitative Characterization of Orientational Order in Liquid Carbon Tetrachloride *J. Chem. Phys.* **2007**, *126*, 164506.
- 65 Bagchi, B. Dynamics of Solvation and Charge-Transfer Dynamics in Liquids. *Ann. Rev. Phys. Chem.* **1989**, *40*, 115-141.
- 66 Stratt, R.M.; Maroncelli, M. Nonreactive Dynamics in Solution: The Emerging View of Solvation Dynamics and Vibrational Relaxation. *J. Phys. Chem.* **1996**, *100*, 12981-12996.
- 67 Fleming, G.R.; Cho, M.H. Chromophore-Solvent Dynamics. *Ann. Rev. Phys. Chem.* **1996**, *47*, 109-134.
- 68 Bedard-Hearn, M.J.; Larsen, R.E.; Schwartz, B.J. Hidden Breakdown of Linear Response: Projections of Molecular Motions in Nonequilibrium Simulations of Solvation Dynamics. *J. Phys. Chem. A* **2003**, *107*, 4773-4777.
- 69 Aherne, D.; Tran, V.; Schwartz, B.J. Nonlinear, Nonpolar Solvation Dynamics in Water: the Roles of Electrostriction and Solvent Translation in the Breakdown of Linear Response. *J. Phys. Chem. B* **2000**, *104*, 5382-5394.
- 70 Laird, B.B.; Thompson, W.H. On the connection between Gaussian statistics and excited-state linear response for time-dependent fluorescence. *J. Chem. Phys.*, **2007**, *126*, 211104.
- 71 Whitnell, R. M.; Wilson, K. R.; Hynes, J. T. Fast Vibrational Relaxation for a Dipolar Molecule in a Polar Solvent. *J. Phys. Chem.* **1990**, *94*, 8625-8628.
- 72 Ki, H.; Choi, S.; Kim, J.; Choi, E.H.; Lee, S.; Lee Y.; Yoon, K.; Ahn, C.W.; Ahn, D.S.; Lee, J.H. et al. Optical Kerr Effect of Liquid Acetonitrile Probed by Femtosecond

1 Time-Resolved X-ray Liquidography. *J. Am. Chem. Soc.*  
2 **2021**, *143*, 14261–14273.

3 <sup>73</sup> Rey, R.; Møller, K.B.; Hynes, J.T. Hydrogen Bond Dy-  
4 namics in Water and Ultrafast Infrared Spectroscopy. *J.*  
5 *Phys. Chem. A* **2002**, *106*, 11993–11996.

6 <sup>74</sup> Laage, D.; Hynes, J.T. Do More Strongly-Bonded Water  
7 Molecules Reorient More Slowly? *Chem. Phys. Lett.* **2006**,  
8 *433*, 80–85.

9 <sup>75</sup> Laage, D.; Hynes, J.T. On the Molecular Mechanism of  
10 Water Reorientation. *J. Phys. Chem. B* **2008**, *112*, 1430-  
11 1442.

12 <sup>76</sup> Laage, D.; Hynes, J.T. On the Residence Time for Water  
13 in a Solute Hydration Shell. Application to Aqueous Halide  
14 Solutions. *J. Phys. Chem. B* **2008**, *112* 7697–7701.

15  
16  
17  
18  
19  
20  
21  
22  
23  
24  
25  
26  
27  
28  
29  
30  
31  
32  
33  
34  
35  
36  
37  
38  
39  
40  
41  
42  
43  
44  
45  
46  
47  
48  
49  
50  
51  
52  
53  
54  
55  
56  
57  
58  
59  
60

TOC graphic

